Inversion of residual motion errors in airborne single and repeat pass interferometry in the presence of squint and large topography variations

Christian Andres, Rolf Scheiber
German Aerospace Center (DLR)
christian.andres@dlr.de, rolf.scheiber@dlr.de

Abstract

The potential and necessity of the estimation and compensation of motion errors beyond the accuracy of up-to-date navigation systems has been demonstrated and proved in several studies during the last years. This paper presents two extensions to an approach based on subaptertures. It extends the so called 'multisquint' algorithm to be used efficiently in cases of big squint angles, large baselines and strong topography variations within the images. The analysis is dedicated to repeat pass interferometry, but also an extension of the inversion to track deviations for single pass systems is presented. In this way, more accurate DEM's can be obtained and increased accuracy for repeat pass interferometric motion compensation can be achieved.

1 Introduction

Algorithms estimating the residual platform deviations, caused by the limited resolution of the navigation systems, from interferometric SAR systems have been developed and refined during the last years. Many applications like differential airborne interferomety show the necessity of estimating those errors. This paper presents some extensions to the proposed algorithms to provide a robust and unsupervised estimation for each kind of interferometric configuration. The extensions are validated using E-SAR data of the German Aerospace Centre (DLR).

1.1 Estimation of residual motion errors

As stated in [2] the phase error, which is induced by the limited accuracy of the navigation systems is averaged along the synthetic aperture during focusing,

$$e_{los} = \int_0^{l_{sa}} \frac{\partial e_y(x)}{\partial x} \cos(\epsilon) + \frac{\partial e_z(x)}{\partial x} \sin(\epsilon)\, dx \quad (1)$$

where ϵ denotes the incidence angle, l_{sa} the length of the synthetic apterure, e_{los} the residual displacement in line of sight and e_y and e_z in airplane geometry. Changing the integration limits in equation 1 by producing azimuth looks leads to the possibility of estimating the residual motion error in line of sight direction as the difference between the phase of of two interferograms, generated with limited bandwidth at different positions of the synthetic aperture, i.e. different azimuth looks

$$\frac{\partial e_{los}}{\partial x} = \frac{\lambda}{4\pi} \frac{\phi^A - \phi^B}{\Delta x} \quad (2)$$

,where the superscripts A and B denote the different looks and Δx represents the distance between the center points of the subapertures along the synthetic aperture. Note, that the residual error in line only repers to the variation of the differential error between master and slave.

1.2 Inversion to airplane geometry

The deviation of the residual estimated in Section 1.1 can be used to refine the flight tracks of the carrier by inverting the equation

$$\frac{\partial e_{los}}{\partial x} = \frac{\partial e_y(x)}{\partial x} \cos(\epsilon) + \frac{\partial e_z(x)}{\partial x} \sin(\epsilon)\,. \quad (3)$$

Because the line of sight error e_{los} can be determined for each range position within one line, equation 3 results in a strong overdetermined problem. In [1] a weighted least squares solution is suggested to perfom a robust inversion of the problem. Finally, the derivatives $\frac{\partial e_y}{\partial x}$ and $\frac{\partial e_y}{\partial x}$ have to be integrated along azimuth to obtain the final track deviations.

2 Single pass interferometry

As demonstrated in [3] residual errors also occurs in single pass systems and can be successfully compensated using the technique presented in section 1.2. After inverting the residual phase errors to airplane geometry the baseline $\overrightarrow{b}$ before estimation can defined as

$$\overrightarrow{b} = \begin{pmatrix} x_s - x_m \\ y_s - y_m \\ z_s - z_m \end{pmatrix} \quad (4)$$

and the refined baseline $\overrightarrow{b'}$ as

$$\overrightarrow{b'} = \begin{pmatrix} x_s - x_m + e_x \\ y_s - y_m + e_y \\ z_s - z_m + e_z \end{pmatrix} \quad (5)$$

. The two displacements e_y and e_z resulting from the line of sight displacement e_{los} can be estimated as shown in the

section before. The residual motion error in flight direction e_x remains unknown, and it is necessary to convert the antenna displacements into attitude angle deviations. Using the assumption that the length of the baseline has to remain constant in the single pass case

$$\left|\overrightarrow{b}\right| = \left|\overrightarrow{b'}\right| \tag{6}$$

leads to an estimation of the residual motion error in flight direction

$$e_x^2 + 2xe_x + e_y^2 + 2ye_y + e_z^2 + 2ze_z = 0 \tag{7}$$

with

$$\begin{aligned} b_x &= x_m - x_s \\ b_y &= y_m - y_s \\ b_z &= z_m - z_s \end{aligned} \tag{8}$$

and

$$\begin{aligned} b_x^{'} &= x_m - x_s + e_x \\ b_y^{'} &= y_m - y_s + e_y \\ b_z^{'} &= z_m - z_s + e_z \end{aligned} \tag{9}$$

.

Equation 7 shows, that two solutions for e_x are possible. Since the residual motion errors are treated to be very small (less than 3cm in repeat pass and even smaller in single pass interferometry), the result with the smaller mean value is chosen.

The attitude angle errors are obtained straight forward by projecting the three baseline coordinates into the planes of the coordinate system.

$$\alpha_{drift} = \arctan\left(\frac{b_y^{'}}{b_x^{'}}\right) - \arctan\left(\frac{b_y}{b_x}\right) \tag{10}$$

$$\alpha_{pitch} = \arctan\left(\frac{b_z^{'}}{b_x^{'}}\right) - \arctan\left(\frac{b_z}{b_x}\right) \tag{11}$$

$$\alpha_{roll} = \arctan\left(\frac{b_z^{'}}{b_y^{'}}\right) - \arctan\left(\frac{b_z}{b_y}\right) \tag{12}$$

The master and the slave image can now be reprocessed using the refined attitude angles to compensate the estimated errors.

3 Squint and Topography

An interesting point is, that the technique to estimate the residual motion errors shows some similarities to a technique to estimate the misregistration of an interferometric image pair presented in [5]. In [5] the coregistration error is derived from the differential phase of two subapertures

$$\Delta t = \frac{\phi_{diff}}{2\pi\left(f_c^A - f_c^B\right)}. \tag{13}$$

Rewriting Equation 13 to

$$\phi_{diff} = \frac{4\pi}{\lambda}\Delta x\left[\sin\left(\theta_{sq}^A\right) - \sin\left(\theta_{sq}^B\right)\right] \tag{14}$$

where $\Delta x = \Delta t v$ shows, that an azimuth misregistration can cause a phase error in the differential phase. This phase error does not cause any problem, as long as it remains constant throughout the scene.

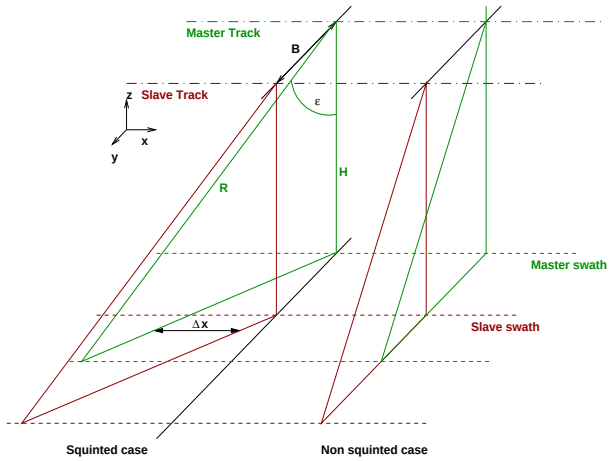

Figure 1: Imaging geometry in airborne repeat pass interferometry for squinted and non squinted case

Figure 1 shows a constant shift in ground range geometry for squinted repeat pass interferometers. This shift, projected to slant range geometry can be expressed as

$$\Delta x = B_{los}\tan\left(\theta_{sq}\right) \tag{15}$$

with

$$B_{los}\left(\epsilon\right) = B_h\sin\left(\epsilon\right) + B_s\cos\left(\epsilon\right), \tag{16}$$

where ϵ denotes the incidence angle of the radar wave to the target. Assuming a low altitude platform like an airplane, the incidence angle cannot be treated as constant throughout range, furthermore it depends on the topography of the scene. Using an external DEM the incidence angle can be written as

$$\epsilon\left(\tau, t\right) = \arcsin\left(\frac{R\left(\tau\right)}{h_{msl} - h_{dem}\left(\tau, t\right)}\right) \tag{17}$$

where τ denotes the time in range and t the time in azimuth direction. The variation of the incidence angle throughout the scene causes a variation of the azimuth misregistration (see Equation 15) which results in a variation of the estimated differential phase.

$$\phi_{diff} = f\left(t, \tau\right) \tag{18}$$

This variation is interpreted as a motion error by the estimation algorithm and causes an overestimation of the residual platform deviations. This effect can be neglected for low squint angles and small baselines but not for flat terrain. In general case of squint, baseline and topography the 2D variation of of Δx must be accounted for very precisely.

4 Experimental results

The testsite chosen for validating the proposed techniques was the Kühtai area close to Innsbruck, Austria. This site is suitable because it shows up more than 1000 meters of topographic variation. Figure 2 shows the digital elevation model of the testsite with overlapped reflectivity.

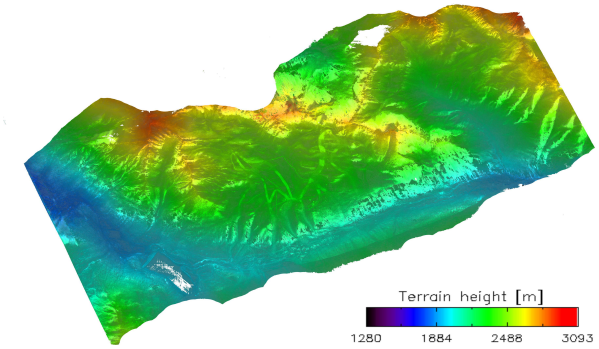

Figure 2: Digital elevation model of Kühtai area with overlapped refrectivity

This DEM was aquired using single pass X-Band interferometry. Additionally repeat pass L-Band scenes with baselines up to 60m were acquired which can be used to demonstrate the topography adaptive shift and to validate the DEM.

4.1 Single pass interferometry

The accuracy of the DEM generated using single pass interferometry is evaluated using a MOSAIC of two scenes, aquired from two different flight directions. Assuming a perfect processing of the images, both DEM's should contain absolutely the same height information. Therefore the difference between the two elevation models in the overlap areas can be used to evaluate the quality of the processing chain.

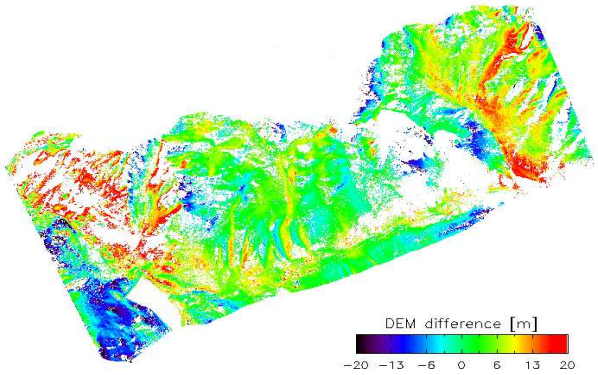

Figure 3: Overlap area using only standard motion compensation to a constant reference level

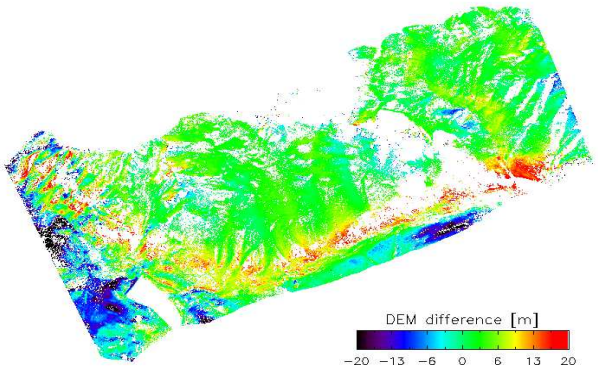

Figure 4: Overlap area using 3 step compensation

Figure 3 shows the overlap area of the scenes processed with motion compensation to a reference level of 2300m. Figure 4 shows the same overlap area processed with the processing chain suggested in [4], using the DEM resulting from the first iteration to compensate topography induced motion errors. Comparing the two figures leads to the conclusion, that accurate, topography dependend, motion compensation, as presented in [6], is also necessary in single pass interferometry. Investigations of areas with obviously uncompensated or wrongly corrected topography correspond to regions of strong layover, at least in one of the two opposite looking scenes. For these layover areas precise consideration of topography is ambigious, and no corrections can be applied by the algorithm.

4.2 Repeat pass interferometry

In repeat pass interferometry a scene with 60m baseline and a squint angle of ≈ -2.6 degrees acquired over Kühtai was chosen. The residual motion errors were estimated and compensated using the 3-step processing chain proposed in [4] with and without considering the variable azimuth shift of equation 15 during the formation of the sub-aperture interferograms.

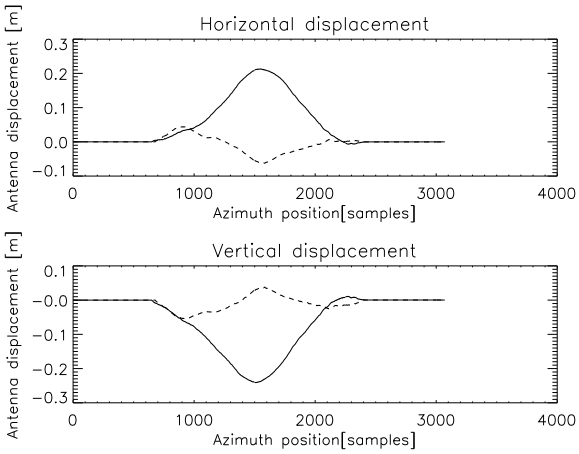

Figure 5: Estimated antenna displacements without (solid line) and with (dashed line) considering the azimuth shift

Figure 5 shows the estimated antenna displacements. Without considering the azimuth shift, an overestimation of $\approx \pm 20$cm is obtained, which is more than the accuracy specifications of the navigation system. Reprocessing the scene with the two estimations leads to coherence images shown in Figure 6.

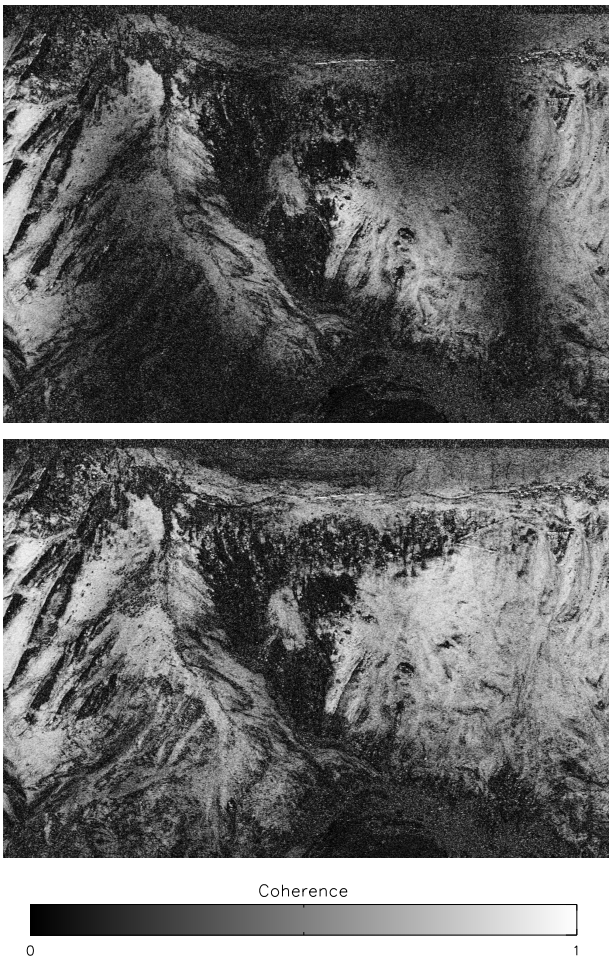

Figure 6: Coherence of the 60m interferogram without (top) and with (bottom) considering the geometry induced azimuth shift during residual motion compensation.

It is obvious, that the overestimation introduces errors in the interferogram, or does not compensate the residual deviations accurately. By considering the misregistration, a much better interferogram is obtained.

5 Conclusions

The combination of squint and large baseline induced azimuth misregistration causes massive overestimation of residual platform deviations even when dealing with "moderate" squint angles lower then 5 degrees. It can further be noted, that the quality of the external DEM has a major impact on the quality of the coherence and the interferometric phase and on the performance of the estimation algorithm. If no external DEM of sufficient quality is available, a refinement of the existing DEM as demonstrated in [3] or in section 4.1 should be performed.
A nice side effect of this work is the approach to generate really accurate DEM's as shown in Figure 3 and 4. Compared to the DEM in Figure 2 it is obvious, that the height error decreases, indicating a good compensation of the topography induced motion errors. However for areas of strong layover, the use of the presented approach is limited and in a further step these regions will be marked as regions with reduced accuracy.
The analysis and improvements presented in this paper are essential for the computation of accurate DEM's in the presence of strong topography variations and for any investigations of airborne differential SAR interferometry in the presence of squint.

References

[1] A. Reigber, P. Prats, and J.J. Mallorqui: *Refined estimation of Time-Varying Baseline Errors in airborne SAR interferometry*,
Proc. IEEE International Geoscience and Remote Sensing Symposium (IGARSS'05), Seoul, Korea, July 25 - 29, 2005

[2] P. Prats, and J.J. Mallorqui: *Estimation of Azimuth Phase Undulations with Multisquint Processing in Airborne Interferometric SAR Images*,
IEEE Transactions on Geoscience and Remote Sensing, vol 41, no. 6, pp. 1530 - 1533, June 2003

[3] P. Prats: *Airborne Differential SAR interferometry*,
Ph. D. Dissertation Universitat Politecnica de Catalunya, November 2005

[4] K. A. C. de Macedo, C. Andres and R. Scheiber: *On the requirements of SAR processing for airborne DInSAR differential interferometry*,
Proc. IEEE International Geoscience and Remote Sensing Symposium (IGARSS'05), Seoul, Korea, July 25 - 29, 2005

[5] R. Scheiber and A.Morreia: *Coregistration of Interferometric SAR Images using Spectral Diversity*,
IEEE Transactions on Geoscience and Remote Sensing, vol 38, No. 5, September 2000

[6] K. A. C. de Macedo, and R. Scheiber: *Precise topography- and aperture-dependend motion compensation for airborne SAR*,
IEEE Geoscience and Remote Sensing Lett., vol 2, No. 2, pp. 172-176, April 2005